Construction and Building Materials 186 (2018) 840–853

Contents lists available at ScienceDirect

Construction and Building Materials

journal homepage: www.elsevier.com/locate/conbuildmat

Interface behavior of tensioned bars embedded in cement-soil mixtures

Changfu Chen [a], Genbao Zhang [a,*], Jorge G. Zornberg [b], Amr M. Morsy [c], Shimin Zhu [a], Hongbo Zhao [a]

[a] College of Civil Engineering, Hunan University, Changsha, Hunan 410082, China
[b] Department of Civil, Architecture and Environmental Engineering, The University of Texas at Austin, Austin, TX 78712, USA
[c] Department of Civil Engineering, Cairo University, Giza 12613, Egypt

HIGHLIGHTS

- A newly designed testing setup and protocol for interface characterization of rebar embedded in cement-soil mixtures.
- A prediction model for interface bond strength by using water-cement ratio and curing time.
- A simplified rebar-mixture interface bond-slip model.
- Recommendations benefiting the design and construction practice.

ARTICLE INFO

Article history:
Received 1 May 2018
Received in revised form 24 July 2018
Accepted 26 July 2018

Keywords:
Pullout test
Interface bond-slip model
Interface bond strength
Deformed bar
Cement-soil mixture

ABSTRACT

The overall performance of reinforced cement-stabilized soils depends significantly on the interface bond mechanisms that develop between the reinforcement and the surrounding cement-soil mixture. A laboratory experimental investigation based on uniform design theory was carried out to characterize the interface behavior of deformed bars embedded in cement-admixed soils. The study focused on the influence of cement content, water content and curing duration on the interface response. The interface bond strength of reinforced cement-soil mixture, as measured in pullout tests, was found to be proportional to the strength of cement-soil matrix, as obtained from unconfined compression tests. A simplified trilinear bond-slip model was developed as part of this study, which when properly calibrated was found to be capable of characterizing the bar-mixture interface shear response. Correlations were obtained to relate the interface bond strength with the three influence factors investigated in this study. The trends obtained on the influence of each factor on the interface bond resistance provided insights that were suitable to guide current design and construction practice of reinforced cement-soil mixture. The results and testing protocols presented in this study facilitated the understanding for interface shear mechanism between deformed bar and cement-soil mixture, and are expected to provide adequate means to satisfy the current lack of bar-mixture interface bond parameters in design specification for reinforced soil mixing structures.

1. Introduction

Cement has been recognized as one of the most important binders/admixtures in geotechnical engineering for ground improvement and stabilization, especially in soft or contaminated clays and sludge [1,2]. Using techniques of soil mixing and jet grouting, cement or slurry can be introduced into the pores of naturally weak soils resulting in pozzolanic reactions forming soil-cement mixtures of improved characteristics [3]. Many research studies were conducted to investigate the improved mechanical and hydraulic properties of cement-stabilized soils, such as strength increase, permeability decrease, and compressibility reduction [4–18].

Stabilized soil systems in some special applications, such as cement mixing columns, are used in excavation support and ground water cut-off solutions, and are unavoidably required to withstand lateral earth pressure [19–22]. This motivation inspired the development of reinforced cement-stabilized soils by introducing reinforcements into cement-soil mixtures. Two different methods are commonly used to introduce reinforcements into cemented soils according to their type. One method uses reinforcements, typically fibers, as additives distributed uniformly over the entire volume of the cemented soil mass to form a composite material with customized cement and fiber contents. This composite material is characterized by a bond interface between fibers and cemented

* Corresponding author.
E-mail address: gbzhang@hnu.edu.cn (G. Zhang).

https://doi.org/10.1016/j.conbuildmat.2018.07.211
0950-0618/

Chen, C., Zhang, G., Zornberg, J.G., Morsy, A.M., Zhu, S., and Zhao, H. (2018). "Interface Behavior of Tensioned Bars Embedded in Cement-Soil Mixtures." Construction & Building Materials, Elsevier, Vol. 186, October, pp. 840-853.

soils, and is reported to exhibit highly improved mechanical properties [23–25]. The second method employs reinforcements as structural elements that bind with the cemented soil mass to resist external loads by mobilizing interface bonds on a specific and continuous interface [26], similar to reinforced concrete. The scope of this study focuses on the bond behavior of this continuous interface, which was specifically formed between the reinforcement rebars and cemented soils, referred to as reinforced cement-soil mixtures. A common application of reinforced cement-soil mixture is Soil Mixed Wall, which was firstly applied in Japan and extensively accepted as a geotechnical solution in soil retention applications [2,27]. Another typical application of reinforced cement-soil mixtures is use with a cement-soil mixing anchor. These anchors can be installed simultaneous with drilling, homing and grouting, unlike the installation of conventional anchors, which requires sequential drilling-homing-grouting procedures. This offsets the difficulty of drilling holes in soft soils. Using this type of anchor can effectively extend the applicability of anchorage techniques to regions characterized by the presence of soft soils [26,28–31].

The pullout resistance of reinforcement embedded in cement-soil mixture depends on the interface shear behavior of the reinforcement and the cement-soil matrix through mechanisms similar to those of reinforced concrete [32]. Structural responses of anchor plates in cement-stabilized backfill and reinforced cement-soil beam were investigated [33,34], whereas studies with exclusive concerns on interface shear response of reinforcement in cement-soil matrix are not yet reported. Consequently, current design specification of reinforced cement-soil structures [26] is deficient in this respect that bond strength of rebar-matrix interface is not considered in the determination of ultimate pullout resistance of reinforcement. It is the case particularly for cement-soil mixing anchor, where the critical role of reinforcement-matrix interface characteristic is emphasized, but relevant quantitative recommendations are not available in design guidelines.

Cement-soil mixture is constituted by four phases, refer to as cementitious solid, soil solid, water and air, typically in condition of being cured for 28 days. As a composite material, it is distinguished from natural soil by the presence of cementitious solid in composition and higher porosity, and from concrete by the introducing cohesive soils instead of cohesionless aggregates [35]. Interface bond strength of reinforcement embedded in soil-cement matrix is gained through cement hardening mechanisms similar to that in concrete matrix. Accordingly, element pullout test used in the characterization of bond performance for reinforced concrete [32,36], is adopted in this study to investigate interface behavior of deformed bar in cement-soil mixture.

It is known that the strength of a cement-soil mixture depends mainly on cement content, water content, and curing period with respect to a certain amount of to-be-treated soft soils [1,11,16]. These three factors were justified to be extensively accounted for in experimental characterization of interface behavior of a certain reinforcement, specifically using deformed bar in this study, embedded in cement-soil matrix. Varying levels are needed for each factor investigated in pullout testing program aiming to obtain their influence patterns on interface bond strength, which thus defines a multi-factor by multi-level experimental program. For a problem with m-factor by n-level, testing program based on full design will lead to a total number of specimens by m^n. While the number of levels is increased in investigation, challenges will be raised substantially in laboratory labor of specimen preparation and consistency control of different specimens. Optimization tools were introduced to implement elaborated design on combination of levels for all factors imposed on each specimen [37,38]. Uniform design theory stands out in these competitive tools by the capability of reducing required specimen quantity substantially from m^n to m with uniformity implied in test results acceptably retained. It should be noted that engineer-accessible uniform design tables are available to identify the level combination of all factors imposed on each specimen. Direct use of these tables eliminates the difficulties in understanding complicated mathematical fundamentals underlying uniform design theory [37]. Reported cases exemplified the applicability of uniform design theory to geotechnical experimental investigations [39–42], and justified the consecutive application to designing this three-factor and multi-level testing program as described earlier.

This study presents an experimental characterization of the interface behavior of a deformed bar embedded in cement-stabilized soils. A number of pullout tests and compression tests were conducted on reinforced cement-soil mixture specimens and cubic cement-soil matrix specimens, respectively. The influence of water content, cement content and curing period on interface shear response was examined through a testing program based on uniform design theory. Interpretations on test results were incorporated into a simplified bond-slip model to characterize interface behavior between reinforcement and cement-soil mixtures. Correlations were developed to associate interface bond strength with testing parameters, of which on basis discussions were conducted to provide insights to current practice of reinforced cement-soil mixture.

2. Testing program

Cement-soil mixture is generally produced in situ by wet/dry soil mixing or jet grouting. Fig. 1a illustrates the phase composition for typical cement-soil mixtures. It is noteworthy that the water content of cement-soil mixture depends on three factors: (a) the method of cement introduction (dry powder or slurry); (b) the moisture condition of the natural soil; (c) the undergoing degree of the hardening process [2]. As shown in Fig. 1b, the influence factors involved in this testing program were defined based on in-situ dry mixing method as follows: (a) water content (C_w), which represents the mass ratio of the added water and the dry soil skeleton; (b) cement content (C_c), also referred to as moist cement content in literature [3], which represents the mass ratio of the cement and the summation of both dry soil skeleton and added water.

Soft clays that are practically suitable for cement stabilization are usually characterized with moisture contents larger than 35% or close to liquid limit. The selection of cement content is optimized such that it provides the best stabilization efficiency, which is soil-specific, with the optimum amount of water based on its availability. In such cases, the optimal cement content is typically less than 30% [3,4,11]. Accordingly, the cement content and water content adopted in this experimental study ranged from 5 to 30% and 45 to 90%, respectively. Cement-stabilized soils were observed to complete hydration and hardening to its full strength in a 90-day curing period. However, strengths with shorter curing periods (e.g. 15 days to 30 days) were commonly applied in design as alternatives due to tight construction schedules in practice [3,43]. Consequently, curing duration (denoted by T_c) adopted in this experimental study ranged from 7 days to 28 days to allow for the evaluation of the interface bond strength increase with time.

The experimental program involved tests conducted at six cement contents, four water contents, and three curing periods, as shown in Table 1. A testing scheme was developed based on the application of uniform design table $U^*12(12^{10})$ [37] to the aforementioned three testing factors, as shown in Table 2. Note that, in $U^*12(12^{10})$, the integer of 12 denotes the required number of levels for each testing factor using this uniform design table, and the integer 10 denotes the maximum number of testing factor applicable to this design table. The number of levels for the three testing factors in this study (Table 1) were extended accordingly

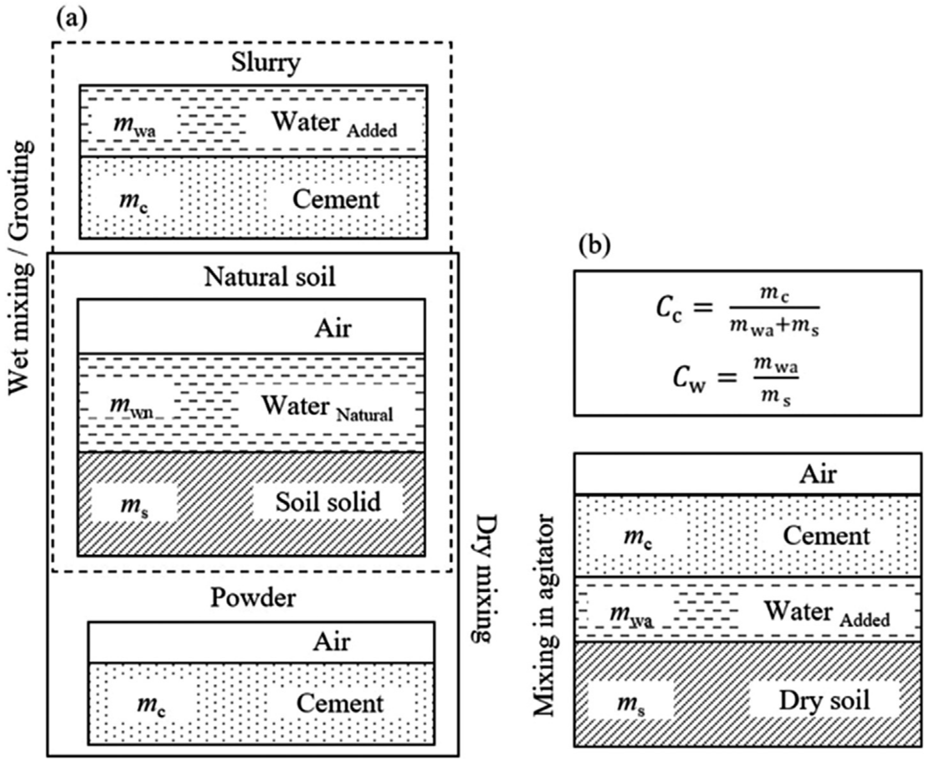

Fig. 1. Schematic of phase composition for typical cement-soil mixture: (a) in-situ production; (b) laboratory preparation in present testing program.

Table 1
Influence factors with respective levels used in testing program.

Influence factor	Number of level	Magnitudes of levels
Cement content C_c (%)	6	5, 10, 15, 20, 25, 30
Water content C_w (%)	4	45, 60, 75, 90
Curing duration T_c (days)	3	7, 14, 28

Table 2
Testing scheme based on uniform design table $U^*12(12^{10})$.

Testing group	C_c	C_w	T_c (days)
TN01	1 (0.05)	6 (0.60)	10 (28)
TN02	2 (0.05)	12 (0.90)	7 (14)
TN03	3 (0.10)	5 (0.60)	4 (7)
TN04	4 (0.10)	11 (0.90)	1 (7)
TN05	5 (0.15)	4 (0.60)	11 (28)
TN06	6 (0.15)	10 (0.90)	8 (14)
TN07	7 (0.20)	3 (0.45)	5 (14)
TN08	8 (0.20)	9 (0.75)	2 (7)
TN09	9 (0.25)	2 (0.45)	12 (28)
TN10	10 (0.25)	8 (0.75)	9 (28)
TN11	11 (0.30)	1 (0.45)	6 (14)
TN12	12 (0.30)	7 (0.75)	3 (7)

Note: *a* (*b*): *a* denotes the level number; *b* denotes the magnitude of this level.

by duplication to their least common multiple to facilitate this direct application of uniform design table.

3. Material properties

Soil samples were collected from flood plain in vicinity of the intersection of Xiangjiang River and Jinjiang River in Changsha, China, which is characterized by the presence of vast soft clay deposits. The collected soil samples were tested to evaluate the soil properties, as shown in Table 3. The results of the particle-size distribution analysis are illustrated in Fig. 2.

Table 3
Materials used throughout testing program.

Properties	Values/Description
Soil sample	
Natural water content (%)	30–70
Liquid limit (%)	58.1
Plasticity limit (%)	28.6
Specific gravity	2.705
Cement	
Type	P.O 42.5
Compressive strength (MPa)	≥42.5 (28-day)
Reinforcement	
Type	HRB 400
Nominal diameter (mm)	16
Rib height (mm)	1.5 ± 0.4
Rib spacing (mm)	10.0 ± 0.5
Yield strength (MPa)	394.7
Young's modulus (GPa)	201

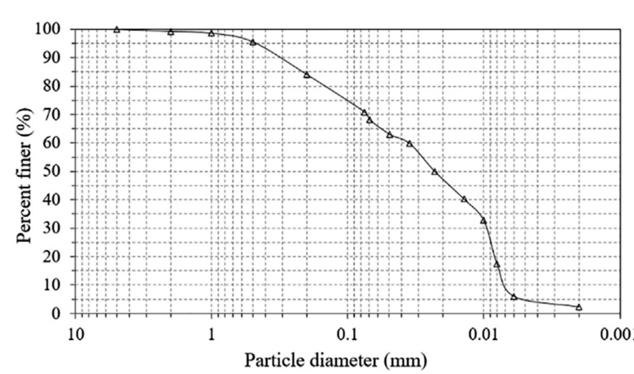

Fig. 2. Particle size distribution curve of soil sample.

It should be noted that natural moisture content of soils in this region ranges from 30 to 70%, and up to 80% or higher in some locations. Cement stabilization was identified to be a very practical ground improvement solution for this soil type [3]. Reinforcement used in the reinforced cement-soil mixture specimens in this experimental study was ordinary deformed reinforced bar [44], as shown in Table 3. The reinforcement sample was 26 cm in length with its loaded end tapped to allow for a screw connection with the pullout loading device. The cement type used in the cement-soil mixture was Ordinary Portland Cement [45], as described in Table 3.

4. Specimen preparation

Natural soil samples were air-dried in laboratory environment at low temperature to avoid the change in the organic component that may occur in oven drying. Soil samples were cleaned from foreign material and were mechanically pulverized. Soil particles passing through 5-mm sieve were preserved in sealed plastic bags with moisture content maintained at 2.1%. Cement-soil mixtures were prepared by mixing specific quantities of soil samples, cement and water in an agitator, according to test configurations (Table 2). Mixing time varied slightly for samples of different water and cement contents, but remained less than 750 s for all samples to reduce specimen inconsistencies involved in the mixing process.

Pullout cells developed by Chen et al. [46–48] were modified to prepare the reinforced cement-soil mixture specimens (Fig. 3). These cells were specially designed to accommodate a reinforcement specimen around which the cement-soil mixture was constituted. Note that the encapsulated length of the reinforcement rebar in the cement-soil mixture in this pullout cell is 8 cm, which represents a segment of a full-scale cement-soil mixing anchor in the field. Pullout tests conducted on anchor elements with comparatively short lengths facilitate the development of interface bond-slip models, as reported in bond behavior characterizations of reinforced concrete and rockbolts [32,49–52]. The ratio of the cement-soil mixture specimen diameter (the interior diameter of the pullout cell) to the reinforcement bar diameter is 12.5 (200:16), which is approximately a full-scale model of a soil-cement mixing anchor cross section in practice [26]. All surfaces in contact with the cement-soil mixture in this setup were coated with petroleum jelly to minimize boundary friction. The lubricated surfaces included the reinforcement sleeves in the cover and base plates, and the inner surface of the cover plate and the side wall (Fig. 3a). A paper sealant was placed on the base plate, and the contact edge of the side wall and the base plate was taped to avoid losses in the specimens in the succeeding vibration phase. It should be noted that pullout tests were conducted without the application of external confining stress. This is because the actual confining mechanism induced by native soils on a cement-soil mixture in the field depends on the interaction that occurs at the native soil-cement-soil mixture interface, which is beyond the scope of this study. The incorporation of a confining mechanism and the interaction between the native soil and cement-soil mixture complicates interpretation of the bond behavior of the cement-soil mixture-reinforcement rebar interface, which is the focus of this study. Consequently, a zero confining stress was adopted at the specimen

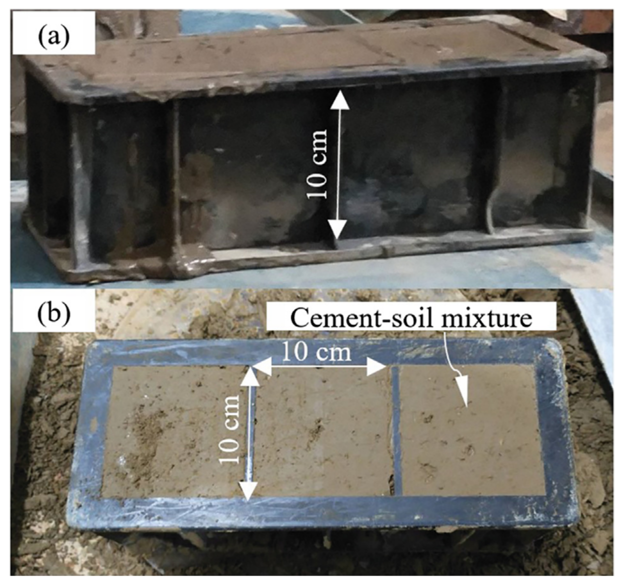

Fig. 4. Cubic cell: (a) view of cells filled with cement-soil mixture; (b) three specimens prepared in a group.

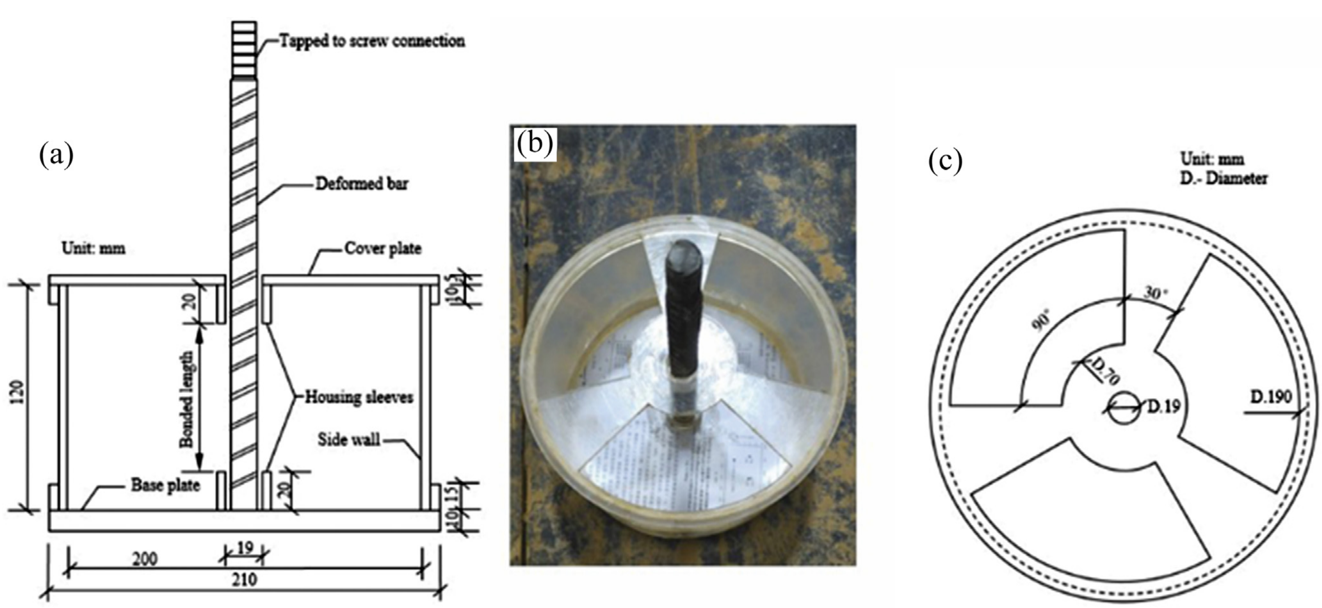

Fig. 3. Pullout cell: (a) schematic of cross-sectional elevation; (b) 3D view of cell; (c) schematic of cross-sectional plan.

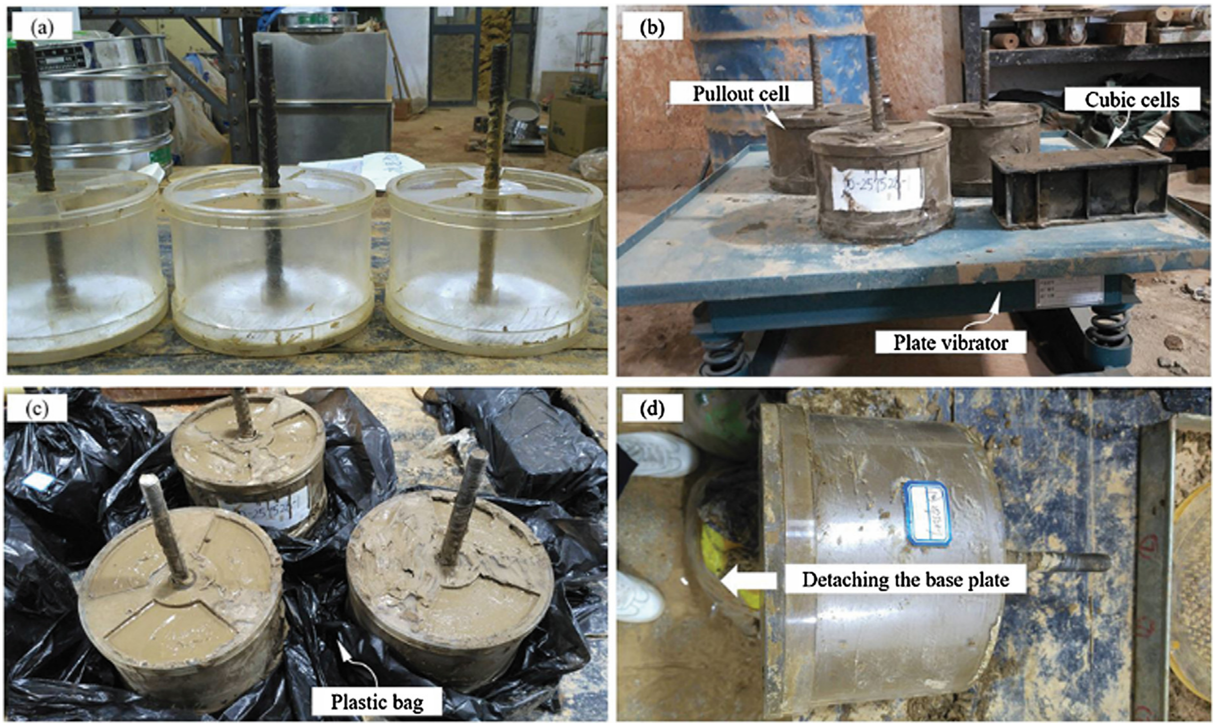

Fig. 5. Specimen preparation: (a) pullout cell with centered bar specimens; (b) densification using a plate vibrator; (c) cement-soil mixtures placed in sealed plastic bags; (d) detaching cover and base plates of pullout cell.

boundaries. Meanwhile, cubic cells were used to prepare the cement-soil mixture specimens for unconfined compression tests, as shown in Fig. 4. The cubic cells were lubricated using a similar method to that used for the pullout cells to facilitate the demolding of specimens (see Fig. 4).

The steel bar specimen was placed vertically into the pullout cells centered in housing sleeves fixed to the base and cover plates (Fig. 5a). Freshly mixed cement-soil mixture was transported into two pullout cells and three cubic cells, and consecutively densified on a plate vibrator for 30 s (Fig. 5b). Vibration is competent to attain a uniform density distribution over the whole volume of cement-soil mixtures, and guarantee the condition of bar-mixture interface free of air bubbles, for specimens with varying fluidities. The cells were placed in sealed plastic bags to preliminary cure for 48 h (Fig. 5c). The cover and base plates were then detached from the pullout cell (Fig. 5d). Both pullout and cubic specimens were sealed again in plastic bags until designated curing durations were reached.

5. Testing procedure

Unconfined compression tests were carried out on cubic specimens by using TYA-2000S Electro-Hydraulic testing machine with load measurement precision of 0.01 kN. The compressive force and its corresponding vertical displacement in compression were not continuously recorded throughout testing. Consequently, only real-time compressive force data could be recorded via the digital panel display, as shown in Fig. 6. The specimens were loaded at a rate ranging from 0.03 to 0.15 kN/second, according to the estimated maximum compression needed in this test. The peak compressive force measured in the loading process was averaged over the cross-sectional area of specimen, which corresponds to the compressive strength of cement-soil mixture (Fig. 6). Meanwhile, pullout tests were carried out on reinforced cement-soil mixture specimens, cured for the same duration as that for cubic

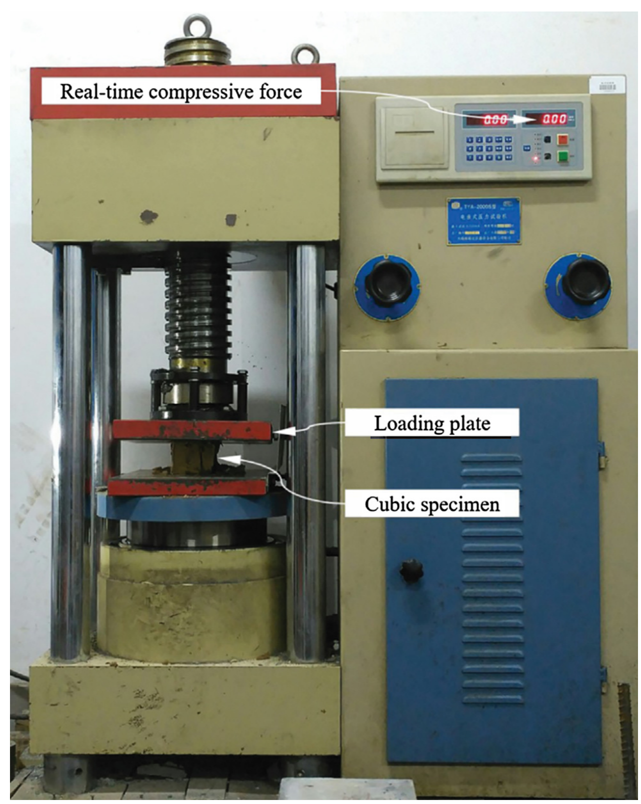

Fig. 6. Unconfined compression test on cubic cement-soil mixture specimen.

specimens, using Frictional Performance Testing System (FPTS), developed by Chen et al. [46,48,53]. A special connection was designed to mount the reinforcement specimen to the loading system. This connection consisted of a two-part hallow cylinder fixed to the load cell using a thread rod, and fixed to the threaded end of the deformed bar specimen using a nut locked inside the cylinder connection, as shown in Fig. 7. The threads in the connection were carefully evaluated to ensure adequate tensile capacity in compliance suitable to sustain the maximum tension provided in FPTS.

With the deformed bar's top end connected to the load cell, the specimen was mounted with the traveling platform of the FPTS using a top plate and fasteners to pull the specimen downward, as shown in Fig. 8. Pullout force is applied to the rebar when the traveling platform moves downward. The load and its corresponding displacement were monitored in real time using a load cell and an LVDT, respectively. The tests were conducted at a constant displacement rate of 1 mm/min. The tests were terminated when pullout displacement reached 20 mm, which guaranteed a complete interface debond between the reinforcement and cement-soil mixture.

6. Experimental results

The shear failure surfaces in the cubic specimens tested in unconfined compression were observed to occur at an angle of approximately 45 degree for all specimens, as shown in Fig. 9. The compressive stress was calculated by dividing the measured compressive force over the area of the cubic specimen to which the compression was applied. The peak compressive stress corresponding to the peak compressive force was used to represent the unconfined compressive strength (UCS) of the cement-soil mixture specimen. For each testing group in Table 2, UCS for

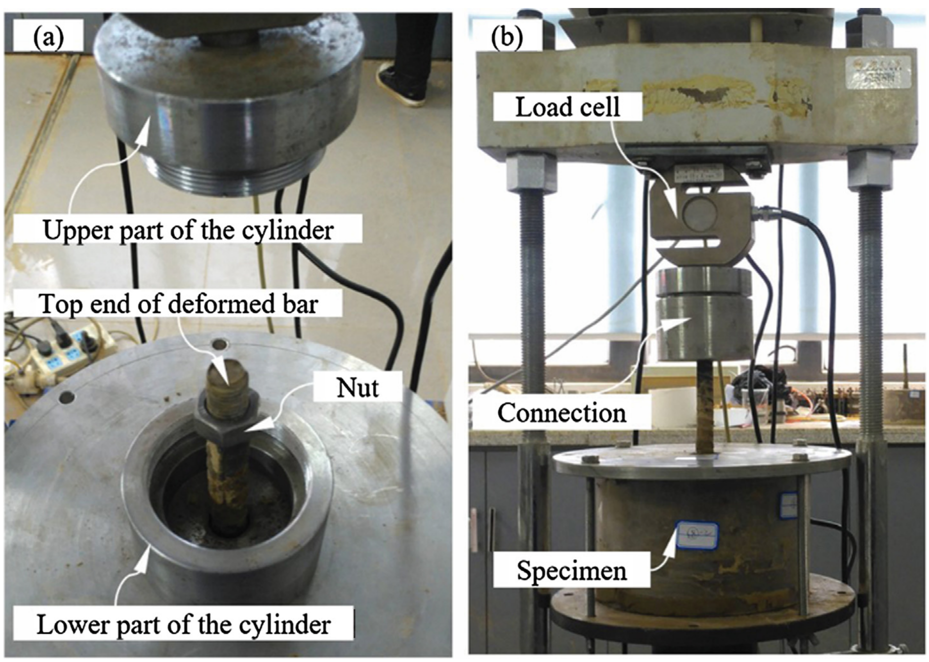

Fig. 7. Connection of specimen and loading system: (a) components of connection; (b) layout with completed connection.

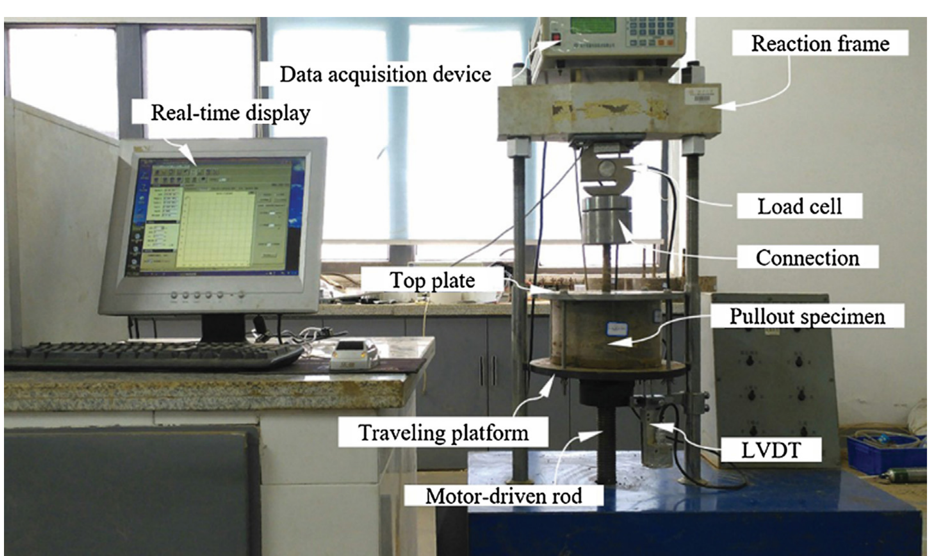

Fig. 8. Setup of pullout test on reinforced cement-soil mixture.

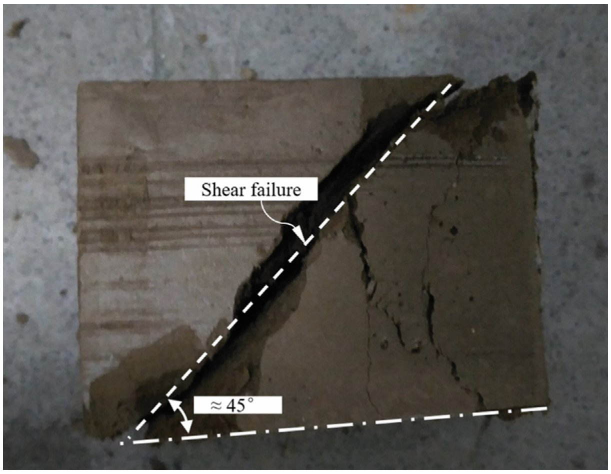

Fig. 9. Front view of cubic specimen showing typical shear failure under compression.

cement-soil mixture prepared at the corresponding testing parameters was determined by a mean value for the three cubic specimens, as shown in Table 4. Consistency of specimens and effectiveness of compression tests were examined by the coefficients of variance (COV) of each testing group, which were smaller than 10%.

Interface bond stresses between the deformed bar and cement-soil matrix were obtained by averaging the pullout force over the entire bond area, assuming uniform distribution of shear stresses. This assumption is deemed valid for reinforcements with short encapsulating lengths [32,49–52]. Interface slips were characterized by the relative displacement between the deformed bar and the cement-soil matrix. This relative displacement was measured by monitoring the displacement of the traveling platform of the loading system (Fig. 8). Note that the tensile strain of the deformed bar is negligible compared to the interface displacement.

Fig. 10 shows the interface shear stress-displacement (bond-slip) curves obtained from the pullout tests for the 12 testing groups involved in this study. Curves from the two tests of the same group were distinguished by suffix -A and -B. The curves were found in a good agreement with minor differences that can be attributed to the variations inherited in material composition, environmental conditions, and laboratory operations despite the effort given to consistently control specimen preparation and testing.

Table 4
Unconfined compressive strength of cement-soil mixture specimens.

Testing group	UCS (MPa)			$\overline{\text{UCS}}$ (MPa)	COV (%)
TN01	–	–	–	–	–
TN02	–	–	–	–	–
TN03	0.59	0.63	0.62	0.61	3.17
TN04	0.30	0.28	0.27	0.28	6.23
TN05	1.62	1.67	1.73	1.67	3.23
TN06	0.51	0.53	0.49	0.51	4.33
TN07	3.06	3.27	3.48	3.27	6.49
TN08	1.77	1.83	1.71	1.77	3.22
TN09	3.99	4.75	4.22	4.32	9.06
TN10	2.72	2.64	3.03	2.80	7.34
TN11	7.41	7.37	6.85	7.21	4.35
TN12	4.15	3.63	3.81	3.86	6.83

Note: "–" denotes unavailable measurements for specimens with very low strength.

A schematic of representative curve in Fig. 10 was illustrated typically in Fig. 11. As shown in Fig. 11, the interface bond-slip relationship can be characterized by three phases: (1) the linear elastic phase, where peak interface bond stress was reached after a small interface displacement (slip) ranging from 0.9 to 2.1 mm; (2) post-peak interface bond stress, which can be defined by strain-softening phase, where the interface bond stress decreased linearly with increasing slip but at a lower rate than that in elastic phase; (3) residual interface bond stress phase, which took place at full interface debond with occurrence of a mechanical climb-slide behavior over rebar ribs, as illustrated by stress fluctuation along with the slip flow. This climb-slide behavior between bar ribs and cement-soil matrix depended on the stiffness and dilatancy properties of the cement-soil mixtures, as well as the geometrical properties of the rebar ribs (not in the scope of this study). Stress jumps were observed immediately after the peak stresses for some specimens (TN03, TN05, TN07, TN08, and TN12), which were also attributed to the climb-slide behavior over the rebar ribs. Note that slip difference between neighboring troughs in the bond-slip curve is equivalent to the rib spacing (10 mm in this testing program), as also depicted in Fig. 11. This validates the occurrence of the climb-slide behavior over the rebar ribs inducing stress fluctuation.

For each interface bond-slip curve, the peak stress was defined as the ultimate interface bond strength (UBS). The stress at the end of the strain-softening phase and before the rib-induced stress climb was defined as the residual interface bond strength (RBS). Table 5 presents the UBS and RBS values obtained for each pullout test, and the average of UBS and RBS values obtained for specimens A and B of each testing group ($\overline{\text{UBS}}$ and $\overline{\text{RBS}}$). It was observed that the interface bond strength increases with increasing cement content, particularly when water content is low, as exemplified by measurements of TN07, TN09 and TN11 shown in Fig. 10. In addition, the interface bond strength tends to decrease with increasing water content, at least for the range of water content involved in this study. This reduction in strength is due to the incomplete pozzolanic reactions occur with excessive water. The full development of interface bond strength for reinforced cement-soil mixtures can be expected at an optimal cement-water ratio, similar to that needed for the full development of the internal shear strength in cement-soil mixtures.

It should be noted that the interface bond strength was obtained in this study by assuming uniformly distributed shear stresses over the entire bond area (i.e., the interface area between the rebar and the cement-soil mixture). In fact, the exact position of essential shear interface is difficult to define in pullout tests because of the existence of a shear band with specific thickness from the interface. This could be illustrated by Fig. 12, which shows the interfacial condition observed on a retrieved rebar.

The magnitude of slip needed to fully mobilize the interface bond strength, i.e. elastic slip limit, can be used in conjunction with interface bond strength to characterize interface elastic modulus. The value of this modulus is a crucial parameter in deformation-involved design of reinforced cement-soil mixtures. A trilinear interface shear constitutive model can be idealized from measured interface bond-slip curves by defining two interface strengths UBS and RBS, as well as their corresponding slip values. Fig. 13 presents the values of elastic slip limit corresponding to the UBS for all pullout specimens. Minor difference between elastic slip limits for parallel specimens in the same testing group further validated the consistency in specimen preparation. It is noteworthy that magnitudes of all elastic slip limits corresponding to the various tests (i.e., various interface bond strengths) fall into a small range between 0.9 and 2.1 mm. The secant stiffness defined by the ratio of the ultimate interface shear strength to the elastic slip limit exhibited no obvious trend. Since the pullout tests conducted in

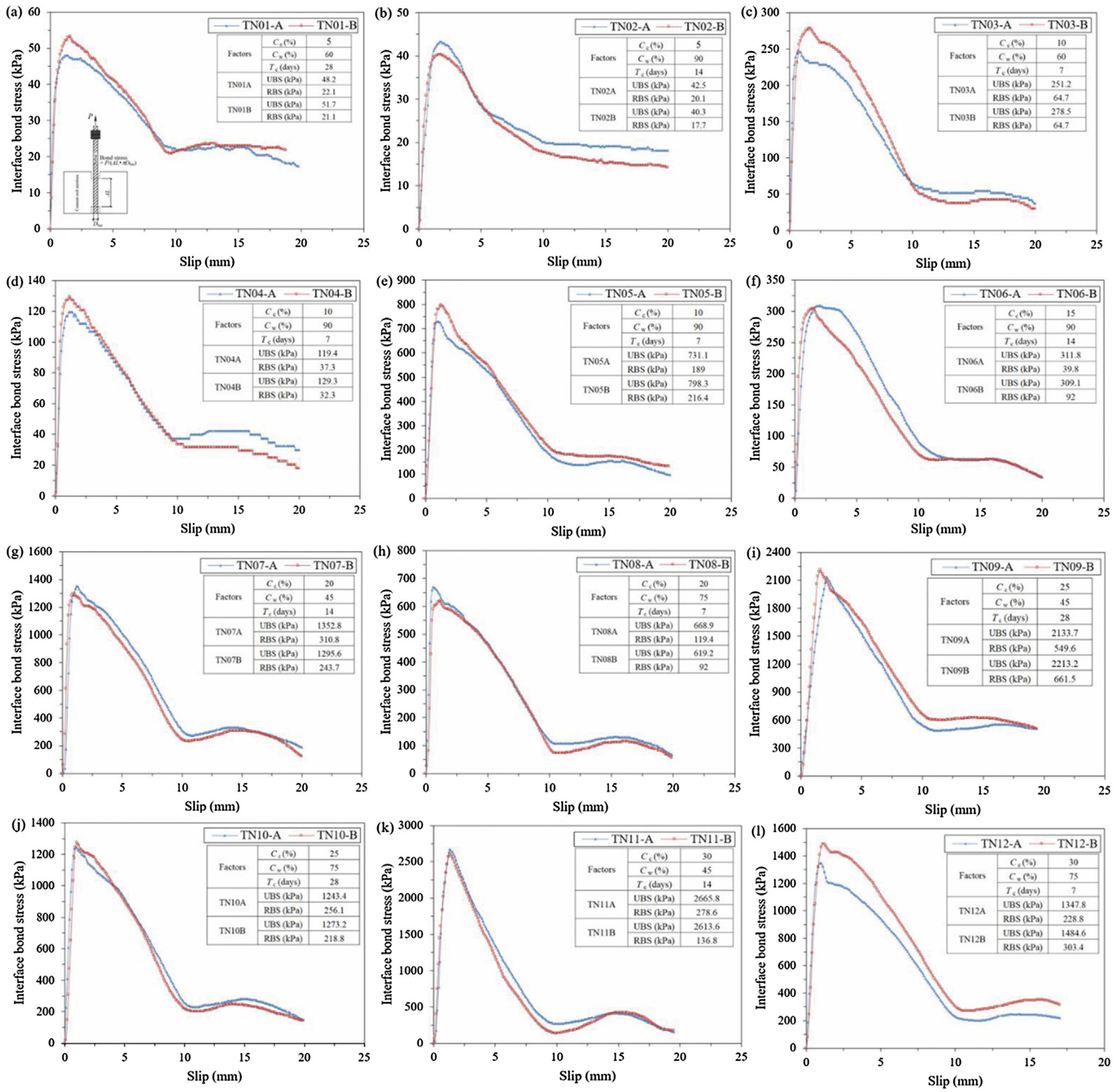

Fig. 10. Interface bond-slip curves from pullout tests: (a) TN01; (b) TN02; (c) TN03; (d) TN04; (e) TN05; (f) TN06; (g) TN07; (h) TN08; (i) TN09; (j) TN10; (k) TN11; (l) TN12.

this study did not provide adequate information about the interface elastic modulus, only the elastic slip limit was used in the development of the interface shear constitutive model between the rebar and cement-soil matrix, as will be discussed later.

7. Regression analyses on test results

The uniformity retained in design of the testing program facilitated the performance of regression analyses, which provided relationships between the controlling parameters involved in this study. Specifically, relationships could be developed between the ultimate interface bond strength and the unconfined compression strength of the cement-soil mixture, between the ultimate and residual interface bond strength, and between the ultimate interface bond strength and the tested influence factors (cement content, water content, and curing time).

7.1. Ultimate interface bond strength ($\overline{UBS}$) versus unconfined compressive strength ($\overline{UCS}$)

Bond strength at the interface between the rebar and cement-soil mixture was found to increase linearly with increasing unconfined compressive strengths of the cement-soil mixture, as shown in Fig. 14, with a determination coefficient $R^2 = 0.957$. The developed linear regression function can be expressed as follows:

$$\overline{\mathrm{UBS}} = 0.402\,\overline{\mathrm{UCS}} \quad (1)$$

The correlation provided a predictive method (without additional laboratory or in situ testing) to determine interface bond strength based on unconfined compressive strength of cement-soil matrix in which a rebar is embedded. The current Chinese specifications [26] can be improved by incorporating recommendations on the relationship between the internal shear

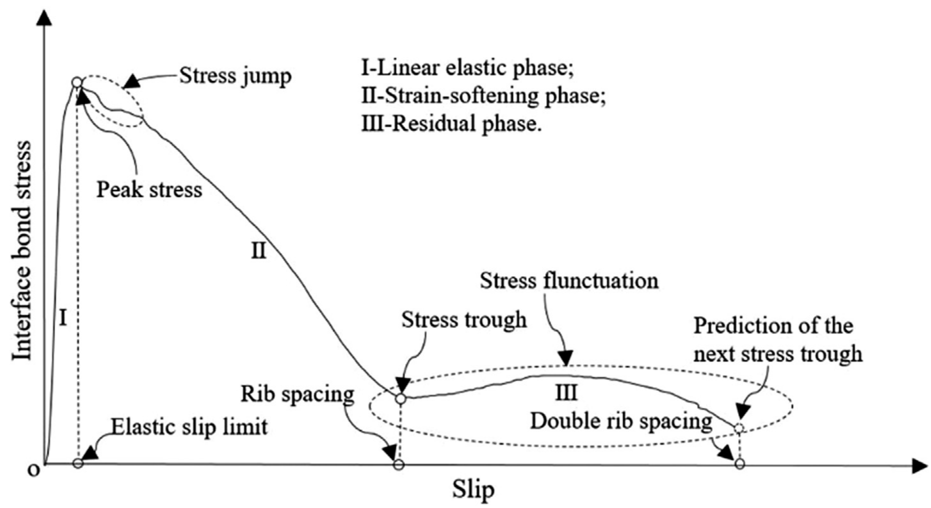

Fig. 11. Schematic of typical interface bond-slip curve.

Table 5
Interface strength measurements of reinforced cement-soil mixtures from pullout tests.

Testing group	Specimen A		Specimen B		$\overline{\text{UBS}}$ (kPa)	$\overline{\text{RBS}}$ (kPa)
	UBS (kPa)	RBS (kPa)	UBS (kPa)	RBS (kPa)		
TN01	48.2	22.1	51.7	21.1	50.0	21.6
TN02	42.5	20.1	40.3	17.7	41.4	18.9
TN03	251.2	64.7	278.5	64.7	264.8	64.7
TN04	119.4	37.3	129.3	32.3	124.3	34.8
TN05	731.1	189	798.3	216.4	764.7	202.7
TN06	311.8	39.8	309.1	92.0	310.5	65.9
TN07	1352.8	310.8	1295.6	243.7	1324.2	277.3
TN08	668.9	119.4	619.2	92.0	644.1	105.7
TN09	2133.7	549.6	2213.2	661.5	2173.5	605.5
TN10	1243.4	256.1	1273.2	218.8	1258.3	237.5
TN11	2665.8	278.6	2613.6	136.8	2639.7	207.7
TN12	1347.8	228.8	1484.6	303.4	1416.2	266.1

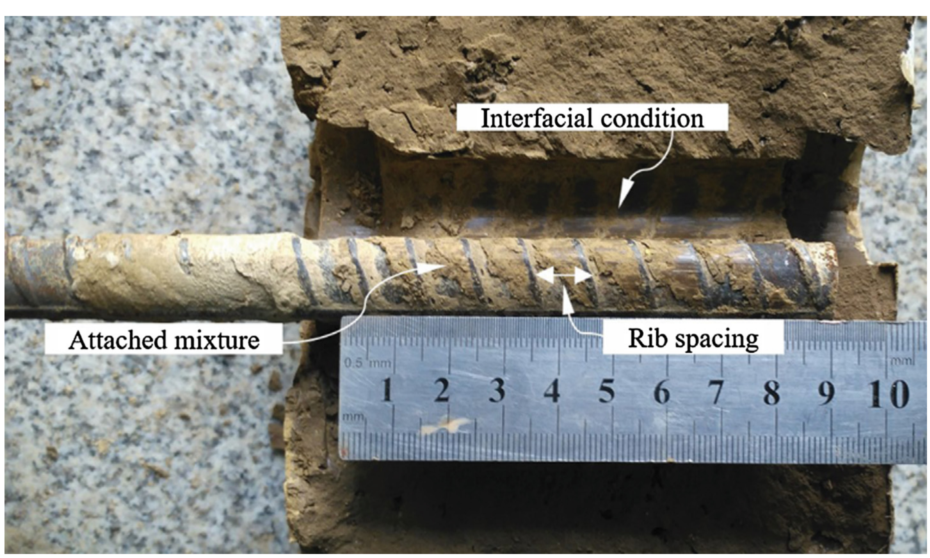

Fig. 12. View of a retrieved rebar and surrounding cement-soil mixture.

strength parameters of cement-soil mixtures and their interface strength parameters with embedded rebar to facilitate design practice. Additional experimental data from further studies is expected to refine this relationship and enrich its reliability.

7.2. Residual interface bond strength (RBS) versus ultimate interface bond strength (UBS)

As explained earlier, residual bond strength of the interface between the rebar and cement-soil mixture characterizes

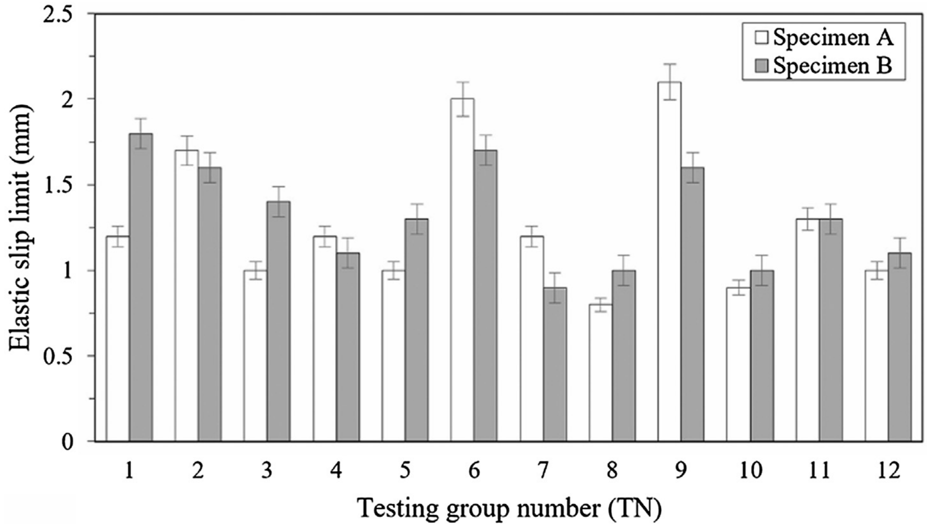

Fig. 13. Magnitudes of elastic slip limit at ultimate interface bond strength.

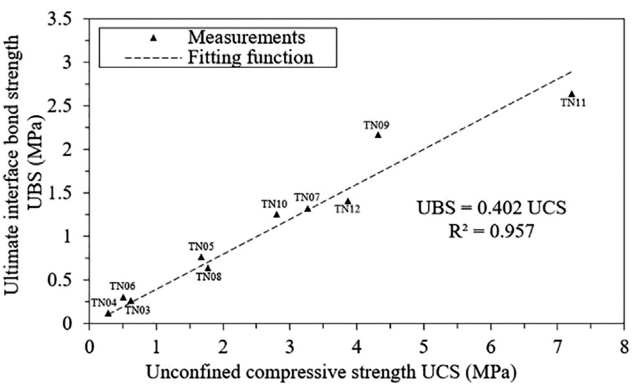

Fig. 14. Relationship of bond strength and unconfined compressive strength.

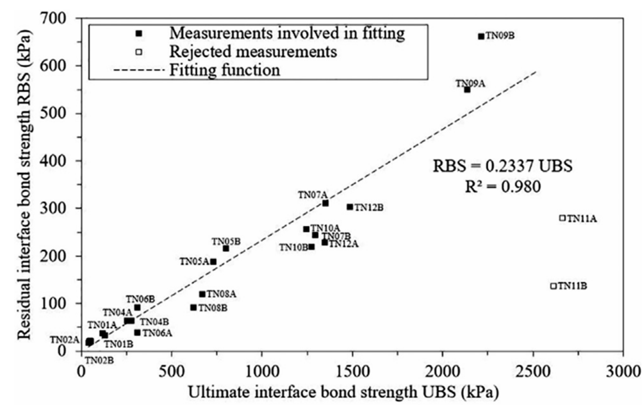

Fig. 15. Residual interface bond strength (RBS) versus ultimate interface bond strength (UBS).

post-debond interface response, which is exclusively induced by frictional resistance, while other bond sources including chemical cohesions along the interface and the internal shear resistance inside the surrounding cement-soil mixture were nearly dissipated in the linear elastic phase and strain-softening phase (Fig. 11). The frictional source, referred to as residual interface bond strength (RBS), has appeared to contribute proportionally to the ultimate bond strength of each individual pullout specimen. This contribution fraction was found to be independent of mechanical properties of surrounding cement-soil matrix, as indicated by proportionally linear function in Fig. 15, which was plotted by fitting on values of RBS versus UBS given in Table 5.

Note that data points from testing group TN11 in Fig. 15 were outliers and were not involved in the regression nor the development of the relationship. It should also be noted that the interface bond-slip curves of TN11 specimens exhibited the most significant stress fluctuation in residual phase compared to other testing groups. This may infer that the combined effect of two mechanical bond mechanisms as occlusion and friction, which occurs in climb-slide behavior over rebar ribs, was not negligible in this case, and that the stress before the fluctuation underestimates the real residual interface bond strength. The developed linear regression between residual interface bond strength and ultimate interface bond strength based on 11 testing groups (22 specimens) can be expressed as follows:

$$\mathrm{RBS} = 0.2337\,\mathrm{UBS} \tag{2}$$

The developed linear regression had $R^2 = 0.980$. While decoupled interface bond interaction mechanism was acknowledged in the scope of this study by assuming that the pre-fluctuation stress trough represents the residual interface bond strength, which was found acceptable, further investigations are needed on the interactions between the cohesion, friction, and occlusion mechanisms to assess the contribution of each mechanism in the development of the interface bond. The residual-to-ultimate interface bond strength ratio can used in the development of the interface bond-slip constitutive model for reinforcement embedded in cement-soil matrix.

7.3. Ultimate interface bond strength as a function of influence factors

It was reported that the strength gain of cement-soil mixtures depends on water-cement ratio (R_{cw}) adopted in the mixing operation [11]. The influence factors tested in this study, cement content (C_c) and water content (C_w), can be related to the cement-water ratio as follows:

$$R_{cw} = \frac{C_w}{C_c(1 + C_w)} \tag{3}$$

Table 6 presents values of R_{cw}, C_c and C_w for each testing group, as well as the corresponding ultimate interface bond strengths ($\overline{\mathrm{UBS}}$, average of measurements for two specimens in the same

Table 6
Bond strength measurements corresponding to influence factor combinations.

Testing group number	Cement-water ratio, R_{cw}	Cement content, C_c (%)	Water content, C_w (%)	Curing duration, T_c (days)	Interface bond strength, $\overline{\text{UBS}}$ (kPa)
TN01	7.5000	5	60	28	50.0
TN02	9.4737	5	90	14	41.4
TN03	3.7500	10	60	7	264.8
TN04	4.7368	10	90	7	124.3
TN05	2.5000	15	60	28	764.7
TN06	3.1579	15	90	14	310.5
TN07	1.5517	20	45	14	1324.2
TN08	2.1429	20	75	7	644.1
TN09	1.2414	25	45	28	2173.5
TN10	1.7143	25	75	28	1258.3
TN11	1.0345	30	45	14	2639.7
TN12	1.4286	30	75	7	1416.2

testing group). Regression analyses was conducted to develop a function for $\overline{\text{UBS}}$ in terms of R_{cw} and the curing duration (T_c) as follows:

$$\overline{\text{UBS}} = 467.984 R_{cw}{}^{-1.697}(\ln T_c + 3.352) \tag{4}$$

Substitution of R_{cw} from Eq. (3) into Eq. (4) leads to a relationship between the ultimate interface bond strength $\overline{\text{UBS}}$ resulting from pullout tests and the tested influence factors, cement content (C_c), water content (C_w), and curing duration (T_c) of cement-soil mixtures. This relationship can be expressed as follows:

$$\overline{\text{UBS}} = 467.984\left(\frac{C_w}{C_c(1 + C_w)}\right)^{-1.697}(\ln T_c + 3.352) \tag{5}$$

The developed relationship in Eq. (5) can be used in the prediction of interface bond strength, which is a critical parameter needed in design practice of reinforced cement-soil mixtures with prescribed material compositions and curing periods. This modeled relationship is particularly useful in reinforced cement-stabilized soil cases in which limited construction periods are allowed, which are usually shorter than curing durations needed to reach adequate mixture strength. The model can be used to facilitate prediction of the interface bond strength based on primary design parameters (cement content and water content), which can be altered to optimize the curing duration and arrive to the desired interface bond strength. Fig. 16 presents the measured interface bond strength data from the implemented testing program against the predicted strength using the developed model to examine the prediction efficiency of the model. By defining the bias as the ratio of prediction and measurement, the magnitude of mean and variance for bias of USB and RSB can be used to examine the predictability of the above correlations, as given in Fig. 16. It was found that the predictions of UBS agree better with measurements in pullout tests than that of RSB. As explained earlier, this difference in predictability of two correlations can be attributed to the ineligible effect of climb-slide behavior on the residual bond strength, which was especially exhibited in the results of TN11. It should be noted that this interface bond strength prediction model was developed for the reinforcement, soil, and cement types used in this study and should be used with caution when applied to other material types.

7.4. Simplified interface bond-slip model

Using the linear correlations obtained between the interface bond strengths (UBS and RBS) and compressive strengths (UCS), various bond stress-slip curves for tested specimens (Fig. 10) could be plotted in the same scale by normalizing the interface bond stresses over the UCS, as shown in Fig. 17. It can be observed that similar trends were exhibited among the bond-slip curves characterizing the interface behavior of reinforced cement-soil mixture specimens, despite having been prepared under different testing conditions. It is suitable to develop a general bond-slip model that captures the common features observed for the specimens typically adopted in this testing program. Fig. 18 presents a trilinear bond-slip model that can be calibrated by utilizing findings to characterize the interface behavior of a tensioned rebar embedded in a cement-soil mixture. This simplified model can be governed by four parameters refer to as ultimate interface bond strength, elastic slip limit, residual interface bond strength and slip at the onset of the residual phase. All these parameters can be calibrated by using reinforcement geometry, material composition

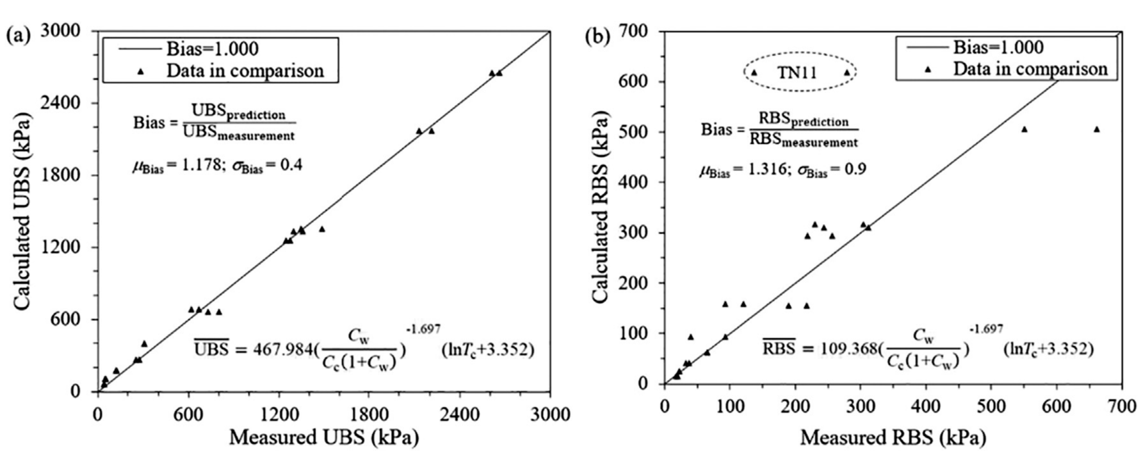

Fig. 16. Examination of predictability of correlations: (a) ultimate interface bond strength from Eq. (5); (b) residual interface bond strength from Eq. (5) and Eq. (2).

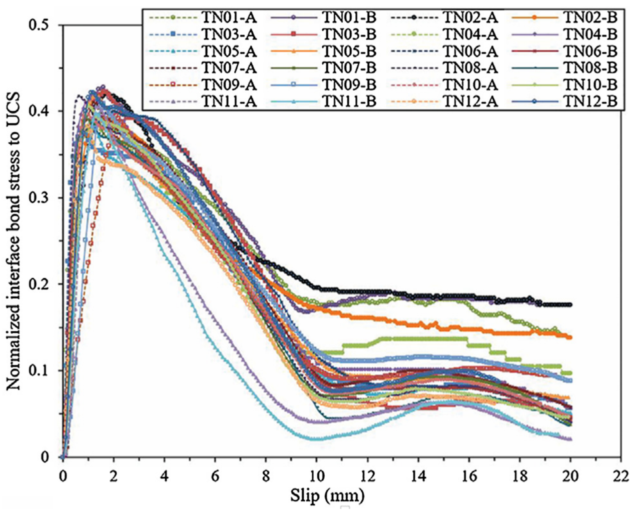

Fig. 17. Normalized interface bond stress versus slip for tested pullout specimens.

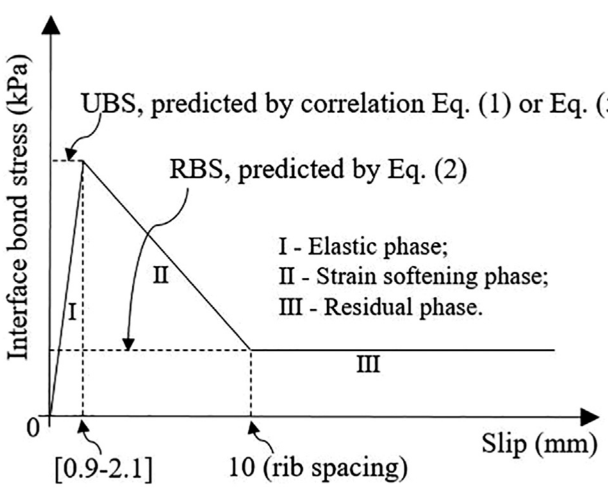

Fig. 18. General bond-slip model characterizing bar-mixture interface.

and the abovementioned relationships. The only unknown is the small range of the elastic slip limit, which can be evaluated by parametric study in specific applications of this model. As stated earlier, this trilinear model was idealized by neglecting interactions between different bonding mechanisms, especially in climb-slide behavior over rebar ribs, which is manifested by stress fluctuation in residual phases of measured interface bond-slip curves. This model can facilitate the understanding of primary interface shear mechanisms that controls the performance of reinforced cement-stabilized soil structures.

8. Discussions

Characterization on bond mechanism of a rebar embedded in cement-soil mixture was facilitated by using correlation associating interface bond resistance with admixed cement amount, natural moisture condition and curing period of mixture. It is common in reinforced cement-stabilization practice that one or two of the influence factors (cement amount, water content and curing time) are constrained limiting the design configuration by varying the remaining factors. For instance, in reinforced cement-soil mixing anchor systems, moisture conditions of natural soils are determined during the site investigation (i.e., constrained water content). If the time for soil mixing is prescribed in a given project (i.e., constrained curing time), then the design variable becomes the amount of cement introduced in soil mixing or jet grouting (i.e., cement content). Accordingly, it is necessary to understand the influence of each factor on the interface bond resistance of the reinforcement embedded in cement-soil mixture, which was investigated using the model developed in this study.

Fig. 19 presents the influence of changing water content on the interface bond strength for conditions with different combinations of cement contents and curing durations. The conditions of the cement-soil mixture are denoted by “c” followed by the cement content and “t” followed by the curing duration in days (e.g., c30t07 denotes 30% cement content and 7-day curing duration). It was observed that the interface bond strength decreases with increasing water content. This reduction in strength with increasing water content is more pronounced in conditions with higher cement content. Natural soils are often characterized by heterogeneous moisture conditions. That is, substantial variation in the interface bond strength along the embedded length of reinforcement could occur unless water content is homogenized. A representative interface bond strength along the reinforcement embedment length is commonly adopted in design practice. This assumed bond strength uniformity should be acceptable in two situations: (1) cement is introduced into soils in the form of slurry, which eliminates natural moist heterogeneity in soils using an external water source, as shown in Fig. 1; and (2) comparatively low cement content is adopted in design where bond strength variation due to moisture variation is insignificant, as shown by curves for cases with c10 in Fig. 19.

Fig. 20 presents the influence of changing cement content on the interface bond strength for conditions with different combinations of water contents and curing durations. The conditions of the cement-soil mixture are denoted by “w” followed by the water content and “t” followed by the curing duration in days (e.g., w45t07 denotes 45% water content and 7-day curing duration). It was observed that the interface bond strength increases exponentially with increasing cement amount. This can be attributed to the increase of cementitious solids inside the cement-soil matrix composition. The influence of cement content on the interface bond strength was found to be more pronounced in cases with comparatively low water contents. It can be explained by the excessive water inducing pore pressure in the hardening process that renders a weak interface micro-structure characterized by large porosity [35]. For soils with high moisture content, it is not necessary to introduce external water source in the soil mixing process to achieve efficient interface bond strengths with reasonable cement consumption. In the current practice, the cement-soil mixing anchor is limited to in-situ jet grouting only [26,31]. However,

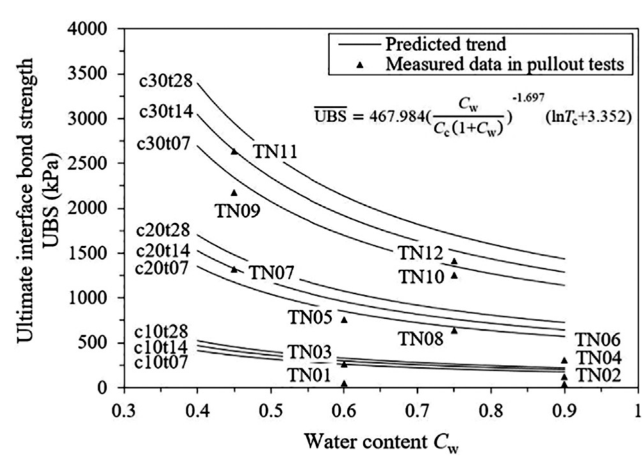

Fig. 19. Influence of water content on interface bond strength.

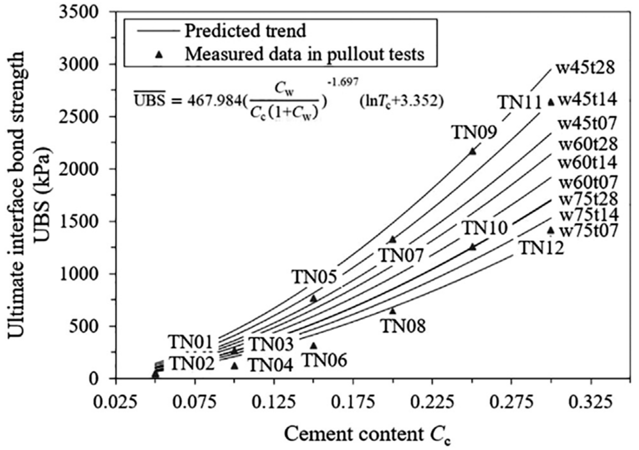

Fig. 20. Influence of cement content on interface bond strength.

reinforcement installation with cement powder instead of slurry can be potentially cost competitive.

Fig. 21 presents the influence of changing curing duration on the interface bond strength for conditions with different combinations of cement and water contents. The conditions of the cement-soil mixture are denoted by "c" followed by the cement content and "w" followed by the water content (e.g., c30w45 denotes 30% cement content and 45% water content). It was observed that varying cement-water ratio can lead to different interface bond strength gain patterns, and ultimately different final strengths (a quasi-constant UBS over time). The interface bond strength gained at a 14-day curing duration (early strength) is usually used in practice as an indicator to the final strength to accelerate construction. This early gained strength can be represented by a fraction of the developed strength over the final strength. Early interface bond strength increases with increasing water-cement ratio. In addition, longer curing durations are needed to fully mobilize the final interface bond strength for mixtures with comparatively high water-cement ratios. While it is acceptable to identify interface bond strength gained over a 90-day curing duration as the final interface bond strength, additional strength may gained after 90 days. This additional strength gain is minor, and it is conservative not to consider it (used as strength backup in design practice). Early interface bond strength is recommended to be used in design for cement-soil mixtures with very low water-cement ratios where strength gain is negligible as indicated by curve c10w75 in Fig. 21.

Provided that sufficient testing data is compiled from further experimental investigations covering a wide range of reinforcement and mixture material properties, an optimized design for reinforced cement-stabilized soils can be developed with reliable accuracy using correlations similar to those developed in this study.

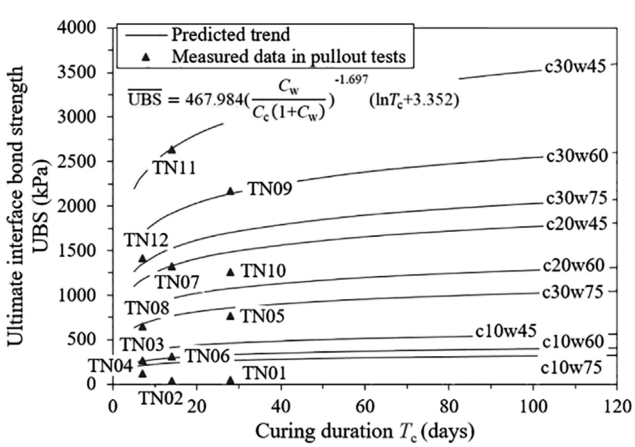

Fig. 21. Interface bond strength increase with curing duration.

9. Conclusions

Laboratory experimental investigation was conducted on the interface bond behavior of a rebar embedded in cement-soil mixtures. A comprehensive testing program was carried out that involved pullout tests on reinforced cement-soil mixture specimens and unconfined compression tests on unreinforced cement-soil mixture specimens. Twelve testing groups were performed with various testing conditions (i.e., various combinations of cement content, water content, and curing duration). Each testing group included two identical specimens to assess the test repeatability. A cell was designed to allow for the preparation of cement-soil mixtures with conditioned cement content, water content, and curing duration. Pullout tests and unconfined compression tests were conducted simultaneously on specimens prepared at the same conditions to obtain bond-slip curves for interfaces between the rebar and the cement-soil mixture, and the corresponding cement-soil mixture compressive strength.

Correlations were developed between ultimate and residual interface bond strength, the mixture compressive strength, and the three influence factors (cement content, water content, and curing duration). Furthermore, a trilinear interface bond-slip model was developed to characterize interface shear behavior of reinforced cement-soil mixture for the materials and conditions involved in this study. The effect of each of the influence factors on the interface bond strength was evaluated and discussed to provide recommendations to the current design practice of reinforced cement-stabilized soils. The conclusions drawn from this investigation can be summarized as follows:

- The newly designed pullout setup and testing protocols were found to be applicable to effectively evaluate the interface bond behavior of a tensioned rebar embedded in cement-stabilized soil with conditioned cement content, water contents and curing duration.
- Ultimate interface bond strength was found to be proportional to the unconfined compressive strength of cement-soil mixture in which the reinforcement was embedded.
- Residual interface bond strength was found to be a fraction of the ultimate interface bond strength. This fraction was found to be independent of testing conditions (cement content, water content, and curing duration).
- The developed relationship between the ultimate interface bond strength and the influence factors (cement content, water content, and curing duration) for reinforced cement-soil mixture can significantly facilitate the design in practice by implementing predictions on the ultimate interface bond strength for any combinations of cement contents, water contents, and curing durations.
- A trilinear interface bond-slip constitutive model can be developed to characterize interface behavior of rebar in cement-soil mixture by using the observations and correlations obtained in this testing program to calibrate the model's relevant governing parameters.
- The assumed uniformly distributed shear resistance along the entire reinforcement embedment length should be carefully adopted by considering moisture content distribution of cement-soil mixture.
- Reinforcement installation technique without introducing external water source into cement-soil mixture is recommended to be considered as a competitive alternative in construction practice.

- Interface bond strength can be reasonably assumed to have fully mobilized after a 90-day curing duration. This recommendation leads to a conservative design.

This study provided insight into interface behavior of reinforcement embedded in cement-stabilized soils, which has been increasingly applied to ground improvement and excavation support in soft soil regions of China. In particular, the presented findings and testing protocols are expected to provide adequate means to supplement the lack of strength parameters for the interface between reinforcement and cement-soil mixture in current design specification of reinforced soil mixing structures.

Acknowledgements

This wok was supported by National Natural Science Foundation of China (grant number 50878082); and China Scholarship Council (grant number 201506130020). The authors appreciate their support. The insightful comments of the reviewers, which enhance essentially the content of this paper, are also gratefully acknowledged by the authors.

References

[1] M. Kitazume, M. Terashi, The Deep Mixing Method, CRC Press, Taylor & Francis Group, Boca Raton, Florida, 2013.
[2] K. Kirsch, A. Bell, Ground Improvement, third ed., CRC Press, Taylor & Francis Group, Boca Raton, Florida, 2013.
[3] J. Han, Principles and Practices of Ground Improvement, John Wiley & Sons, Inc., Hoboken, New Jersey, 2016.
[4] R. Babasaki, M. Terashi, T. Suzuki, A. Maekawa, M. Kawamura, E. Fukazawa, Japanese Geotechnical Society Technical Committee Report: factors influencing the strength of improved soil, in: R. Yonekura, M. Terashi, M. Shibazaki (Eds.), Grouting and Deep Mixing: Proceedings of the 2nd International Conference on Ground Improvement Geosystems, Balkema Publishers, Tokyo, Japan, 1996, pp. 913–918.
[5] K.Q. Lin, I.H. Wong, Use of deep cement mixing to reduce settlements at bridge approaches, J. Geotech. Geoenviron. Eng. 125 (4) (1999) 309–320.
[6] M. Terashi, The state of practice in deep mixing methods, ASCE Geotechnical Special Publication 120 (2003) 25–49.
[7] S. Horpibulsuk, N. Miura, T. Nagara, Assessment of strength development in cement-admixed high water content clay with Abrams' law as a basis, Géotechnique 53 (4) (2003) 439–444.
[8] S. Horpibulsuk, R. Rachan, A. Suddeepong, State of the art in strength development of soil–cement columns, Proc. Inst. Civ. Eng.-Ground Improvement 165 (4) (2012) 201–215, https://doi.org/10.1680/grim.11.00006.
[9] S.H. Chew, A.H.M. Kamruzzaman, F.H. Lee, Physicochemical and engineering behavior of cement treated clays, J. Geotech. Geoenviron. Eng. 130 (7) (2004) 696–706.
[10] S. Larsson, H. Stille, L. Olsson, On horizontal variability in lime-cement columns in deep mixing, Géotechnique 55 (1) (2005) 33–44.
[11] H. Åhnberg, Strength of Stabilized Soils-A Laboratory Study on Clays and Organic Soils Stabilized with Different Types of Binder PhD Thesis, Lund University, Sweden, 2006.
[12] N.C. Consoli, G.V. Rotta, P.D.M.A. Prietto, Yielding-compressibility strength relationship for an artificially cemented soil cured under stress, Géotechnique 56 (1) (2006) 69–72, https://doi.org/10.1680/geot.2006.56.1.69.
[13] S.L. Shen, J. Han, Y.J. Du, Deep mixing induced property changes in sensitive marine clays, J. Geotech. Geoenviron. Eng. 134 (6) (2008) 845–854.
[14] S. Pongsivasathit, J.C. Chai, W.Q. Ding, Consolidation settlement of floating-column-improved soft clayey deposit, Ground Improvement 166 (GI1) (2013) 44–58.
[15] H.W. Xiao, F.H. Lee, An energy-based isotropic compression relation for cement-admixed soft clay, Géotechnique 64 (5) (2014) 412–418, https://doi.org/10.1680/geot.13.T.019.
[16] M.J. Timoney, B.A. McCabe, A.L. Bell, Experiences of dry soil mixing in highly organic soils, Proc. Inst. Civ. Eng.-Ground Improvement 165 (1) (2012) 3–14.
[17] M.J. Timoney, Strength verification methods for stabilized soil-cement columns: a laboratory investigation of PORT and PIRT, Ph.D. thesis, NUI Galway, 2015.
[18] M.J. Timoney, B.A. McCabe, Strength verification of stabilized soil-cement columns: a laboratory investigation of the push-in resistance test (PIRT), Can. Geotechnical J. (2017), https://doi.org/10.1139/cgj-2016-0230.
[19] J. Han, S. Oztoprak, R.L. Parsons, J. Huang, Numerical analysis of foundation columns to support widening of embankments, Computer and Geotechnics 34 (6) (2007) 435–448.
[20] J.C. Chai, N. Miura, T. Kirekawa, T. Hino, Settlement prediction for soft ground improved by columns, Ground Improvement 163 (G12) (2010) 109–119.
[21] Y. Jiang, J. Han, G. Zheng, Numerical analysis of consolidation of soft soils fully-penetrated by deep-mixed columns, KSCE J. Civ. Eng. 17 (1) (2013) 96–105.
[22] S. Shen, Z. Wang, J. Yang, C. Ho, Generalized approach for prediction of jet grout column diameter, J. Geotech. Geoenviron. Eng. 139 (12) (2013) 2060–2069.
[23] B. Fatahi, H. Khabbaz, B. Fatahi, Mechanical characteristics of soft clay treated with fiber and cement, Geosynthetics Int. 19 (3) (2012) 252–262, https://doi.org/10.1680/gein.12.00012.
[24] B. Fatahi, T.M. Le, B. Fatahi, H. Khabbaz, Shrinkage properties of soft clay treated with cement and geofibers, Geotech. Geol. Eng. 31 (2013) 1421–1435, https://doi.org/10.1007/s10706-013-9666-y.
[25] L. Nguyen, B. Fatahi, Behavior of clay treated with cement & fiber while capturing cementation degradation and fibre failure – C3F model, Int. J. Plasticity 81 (2016) 168–195, https://doi.org/10.1016/j.ijplas.2016.01.015.
[26] CECS 147, Technical Specification for Soil Mass with Reinforced Cement Soil Pile and Anchors, China Planning Press, Beijing, China, 2016.
[27] G. Zhang, Y. Xu, D. Fu, Testing study and application of shape steel pullout in SMW construction method, China J. Rock Mech. Eng. 21 (3) (2002) 444–448.
[28] Q. Liu, Y. Yang, Stability analysis of inclined anchorage pile for reinforced cement-soil in bracing excavation structure and its application, China J. Rock Mech. Eng. 24 (S2) (2005) 5331–5336.
[29] G. Liu, R. Ye, X. Shen, C. Shen, Mechanisms of cement-soil mixing anchor and application in foundation pit support project, Chinese J. Geotech. Eng. 32 (S2) (2010) 363–366.
[30] G. Liu, X. Shen, Z. Su, L. Lu, Improvement test of uplift resistance and deformation of cement-soil mixing anchor, Rock Soil Mech. 32 (S1) (2011) 78–82.
[31] H. Xu, L. Chen, J. Deng, Uplift tests of jet mixing anchor pile, Soils and Foundations 54 (2) (2014) 168–175.
[32] CEB Task Group Bond Models, Bond of Reinforcement in Concrete, International Federation for Structural Concrete, Lausanne, Switzerland, 2000.
[33] N. Yu, H. Zhu, R. Liang, Experimental study on mechanical properties of reinforced cemented-soil, China Civ. Eng. J. 37 (11) (2004) 78–84.
[34] N.C. Consoli, C.A. Ruver, F. Schnaid, Uplift performance of anchor plates embedded in cement-stabilized backfill, J. Geotech. Geoenviron. Eng. 139 (3) (2013) 511–517.
[35] Y. Liu, J. Hu, H.W. Xiao, E.J. Chen, Effects of material and drilling uncertainties on artificial ground freezing of cement-admixed soils, Can. Geotech. J. 54 (2017) 1659–1671, https://doi.org/10.1139/cgj-2016-0707.
[36] A.R.V. Wolenski, S.S. De Castro, S.S. Penna, R.L.A. Pitangueira, B.V. Silva, M.P. Barbosa, Experimental and finite element analysis of bond-slip in reinforced concrete, Ibracon Struct. Mater. J. 8 (6) (2015) 787–799, https://doi.org/10.1590/S1983-41952015000600004.
[37] K.T. Fang, Uniform Design and Uniform Design Tables, Science Press, Beijing, China, 1994.
[38] K.T. Fang, R. Li, A. Sudjianto, Design and Modeling for Computer Experiments, CRC Press, New York, 2006.
[39] S. Mei, Q. Sheng, X. Feng, Application of uniform design to geotechnical engineering, Chin. J. Rock Mech. Eng. 23 (16) (2004) 2694–2697.
[40] G. Chen, S. Cheng, Y. Lu, D. Chen, Sensitivity analysis of slope stability based on uniform design, J. Hydraulic Eng. 37 (11) (2007) 1397–1401.
[41] J. Song, Z. Song, R. Sun, Study of uniform experiment design method applying to civil engineering, International Conference on Advances in Computational Modeling and Simulation, Procedia Eng. 31 (2012) 739–745.
[42] X. Huang, W. Gong, B. Mu, T. Huang, R. Xie, Study of bearing performance of steel pipe settlement reducing pile with pile cap based on uniform design, Rock Soil Mech. 35 (11) (2014) 3149–3155.
[43] JGJ 79, Technical Code for Ground Treatment of Buildings, China Planning Press, Beijing, China, 2012.
[44] GB 1499.2, Steel for the Reinforcement of Concrete-Part 2: Hot Rolled Ribbed Bars, Standard Press of China, Beijing, China, 2007.
[45] GB 175, Common Portland Cement, Standard Press of China, Beijing, China, 2007.
[46] C. Chen, G. Liang, Y. Tang, Y. Xu, Anchoring solid-soil interface behavior using a novel laboratory testing technique, Chin. J. Geotech. Eng. 37 (6) (2015) 1115–1122. https://doi.org/10.11779/cjge201506018.
[47] C. Chen, G. Liang, et al., A device and method for preparing soil samples used in testing frictional performance of anchor/pile-soil interface, China Patent ZL 2014 1 0176979.8, filed April 29, 2014, and issued July 6, 2016.
[48] C. Chen, G. Zhang, J.G. Zornberg, X. Zheng, Element nail pullout tests for prediction of soil nail pullout resistance in expansive clays, Geotech. Testing J., accepted, 2018, in press.
[49] B. Benmokrane, A. Chennouf, H.S. Mitri, Laboratory evaluation of cement-based grouts and grouted rock anchors, Int. J. Rock Mech. Mining Sci. Geomech. Abstracts 132 (7) (1995) 633–642.
[50] L.B. Martin, M. Tijani, F. Hadj-Hassen, A new analytical solution to the mechanical behavior of fully grouted rockbolts subjected to pull-out tests, Constr. Build. Mater. 25 (2011) 749–755.
[51] S. Ma, J. Nemcik, N. Aziz, An analytical model of fully grouted bolts subjected to tensile load, Constr. Build. Mater. 49 (2013) 519–526.
[52] S. Ma, J. Nemcik, N. Aziz, Z. Zhang, Numerical modelling of fully grouted rockbolts reaching free-end slip, Int. J. Geomech. 16 (1) (2016) 04015020.
[53] C. Chen, G. Liang, et al., A testing system and method for frictional performance of anchor/pile-soil interface, China Patent ZL 2014 1 0176877.6, filed April 29, 2014, and issued March 30, 2016.